Journal of Population Therapeutics & Clinical Pharmacology

RESEARCH ARTICLE
DOI: 10.53555/vd8sjh61

FLUORESCENCE QUENCHING BASED SENSING OF MERCURY ION USING QUINOLINE BASED NANOPROBE

A. A. Kamble[1*]

[1*]Assistant professor, Department of chemistry, Padmabhushan Vasantraodada Patil Mahavidyalaya, Kavathemahankal

***Corresponding author:** A. A. Kamble
*Assistant professor, Department of chemistry, Padmabhushan Vasantraodada Patil Mahavidyalaya, Kavathemahankal

Abstract:
The reprecipitation technique was utilized to prepare organic nanoparticles of 8-hydroxyquinoline, which were then employed for the detection of Hg^{2+} ions in aqueous solutions via fluorescence quenching. The formation of the organic nanoparticles was confirmed using UV-Visible spectroscopy, fluorescence spectroscopy, and dynamic light scattering techniques. The extended lifetime of the nanoparticle suspension indicates their formation through aggregation. The prepared nanoparticle suspension demonstrated high selectivity for Hg^{2+} ions in the presence of other cations. The developed method was also applied to detect Hg^{2+} ions in real environmental samples, with a limit of detection of 0.6920 µg/mL. The Stern-Volmer plot showed excellent linearity for Hg^{2+} ion concentrations ranging from 0 to 6 µg/mL, with an R^2 value of 0.990.

1. Introduction:

In most recent years, organic nanoparticles (ONPs) have attracted much attention in nanoscale science and engineering technology due to their peculiar chemical and physical properties such as novel electronic and optical.[1,2] Their major application areas include catalysts, absorbents, chemical and biological sensors, optoelectronics, information storage, photonic and electronic devices.[3,4] Over past few years, ONPs have drawn a great importance due to its different chemical and physical behavior from their corresponding bulk materials and it also shows innumerable applications in the practical world.[5,6] In comparison to other ONPs, the functionalized nanoparticles shows an immense desirability around the world in recent years[7, 8], as they have a broad absorption band in the visible region of electromagnetic spectrum.[9–12] To the best of our knowledge, ONPs particularly functionalized nanoparticles have recently been the focus of great interest because the fluorescence property which is strongly dependent on size and shape of the particle, the adsorbed species, dielectric properties of the medium, and inter-particle distances between them.[13] This unique properties of ONPs helps them to use as an analytical probes in biotechnological and chemical system such as colorimetric sensors for metal ions.[14-15] In particular, the 8-hydroxyquinoline nanoparticles (HQNPs) shows distinctive optical and electric properties and therefore they have been found wide applications for analytical purposes.

The environmental contamination with heavy metal ions has been an important concern throughout the world for decades. Toxic heavy metal ions has received much attention due to its high toxicity and bioaccumulative properties, and its toxic pollutants exerts lethal hazard and adverse effects on the environment and human beings.[16–18] In comparison to other metal ions, Hg^{2+} is one of the most toxic

elements on the planet, second after to plutonium, and is considered as one of the most dangerous metal ions for environment and human health. Environmentally, the emission of mercury and their contamination with ecosystems occurs through a variety of natural and anthropogenic sources, including oceanic and volcanic emissions, gold mining, solid waste incineration and the combustion of fossil fuels.[19] Hg^{2+} is widely distributed in air, water, and soil and it is a toxic element that exists in metallic, inorganic, and organic forms.[20] The most stable form of inorganic mercury is mercuric ion (Hg^{2+}), which has high water solubility so always remains in surface water and long exposure of it causes health problems such as damage to the brain, nervous system, kidneys, and endocrine system.[21, 22] In aqueous solution, bacteria converts water-soluble Hg^{2+} to methyl mercury, which subsequently bioaccumulates through the food chain.[23] Methyl mercury is known to cause health problems such as sensory, motor, and neurological damage. It is particularly dangerous for children, because it can causes several serious developmental delays.[24] Hg^{2+} shows strong affinity towards the ligands containing sulfur group and causes the blocking of sulphydryl groups of proteins, enzymes, membranes and it damage to the central nervous system, DNA, mitosis and the endocrine system.[25] Focusing on its serious hazardous effects to human health and environment, it is very necessary to build a simple, inexpensive, and high performance method to determine Hg^{2+} with high selectivity in aqueous solution.

To date, numerous methods have been reported for the determination of Hg^{2+} including colorimetry,[26,27] spectrophotometry,[28] atomic absorption spectrometry,[29] stripping voltammetry,[30] inductively coupled plasma atomic emission spectrometry,[31] high-performance liquid chromatography,[32] ion selective electrode (ISE) and flame photometry,[33] however their excellent results is achieved at the cost of expensive instrumentation and time-consuming sample preparation and preconcentration procedures.[34] Nowadays, fluorimetric sensors are gaining increased attention due to their simplicity, rapidity, high selectivity and ease of measurement. Compared to other assays, fluorimetric sensors allow direct and on-site analysis of the sample. Among them, (HQNPs) based fluorimetric sensors have many advantages over other nanoparticles-based ones, as they have higher extinction coefficients and lower prices, allowing detection with minimal consumption of material.[35] Thus it can be easily implemented in day-to-day laboratory practices.

Herein, a highly selective fluorimetric assay is proposed for the detection of Hg^{2+} in aqueous solution using HQNPs as a chemosensors based on inducing aggregation. We prepared the HQNPs by a simple reprecipitation method. Fluorescence intensity of HQNPs is extremely quenched by Hg^{2+} without significant shift in the λ_{max} without interferences from common ions. The reason of fluorescence intensity quenching lies in the formation of amalgam like structure between HQNPs and Hg^{2+}.[36] This is due to the merging of Hg^{2+} in to the surface of HQNPs resulting in the fluorescence quenching. Furthermore the proposed method was successfully applied for determination of Hg^{2+} from water samples collected from different sources in the campus in a complex matrix without pretreatment by standard addition method. This probe offers the advantages of simplicity, selectivity, reproducibility and good stability, which makes it a valuable pathway for analytical purposes. The easy synthesis and high stability of the HQNPs allow the method to be very simple and easy to implement.

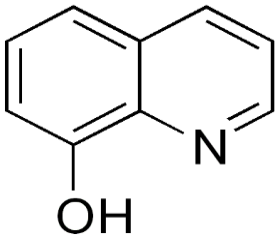

Structure of 8-hydroxyquinoline

2. Experimental:

2.1 Materials:

8-hydroxyquinoline and mercury chloride ($HgCl_2$) obtained from Sigma Aldrich, Mumbai, were used as received. Analytical Grade acetone (S. D. Fine Chemicals, Mumbai) was used after distillation.

The ultrapure water obtained by passing distilled water through Millipore unit (India) was used in all experiments.

2.2 Preparation of 8-hydroxyquinoline nanoparticles:

Suspension of 8-hydroxyquinoline nanoparticles were prepared by a simple reprecipitation method. 1ML solution of perylene in acetone (1.3 mM) was injected by microsyringe into 50 ml aqueous solution (25 mM) with vigorous stirring. The mixture was sonicated for about 30 min at 30^0 C and nanoparticles dispersed into water were obtained. 8-hydroxyquinoline nanoparticles having narrow size distribution and smaller size were undertaken for detailed characterization.

2.3 Characterization Techniques:

The size of 8-hydroxyquinoline nanoparticles was measured on Malvern Zetasizer (nano ZS-90) equipped with a 4 mW, 633nm He-Ne Laser (U.K.) at 25^o C under fixed angle of 90^{o}C in disposable polystyrene cuvettes. The steady state fluorescence emission spectrum of the aqueous dispersion of 8-hydroxyquinoline nanoparticles was collected using a Spectrofluorimeter (JASCO, Japan, Model FP- 8300). The time resolved fluorescence measurements were carried out under ambient condition ($\lambda_{ex}/\lambda_{em}$=380nm/565nm) using a Time-Correlated Single-Photon Counting (TCSPC) spectrometer (Horiba, Japan). Absorption spectra were recorded on (UV-3600 UV-Visible-NIR Spectrophotometer, SHIMADZU Japan). Scanning Electron Microscope (JEON-6360 Japan) was adopted to examine the morphology and size of nanoparticles.

3 Results and Discussion:

3.1 Particle size and morphology of 8-hydroxyquinoline nanoparticles:

Figure 1 shows the particles size distributions of 8-hydroxyquinoline nanoparticles in aqueous suspension obtained from DLS record. The size distribution of nanoparticles is remarkably narrow and average diameter of nanoparticles is 20 nm.

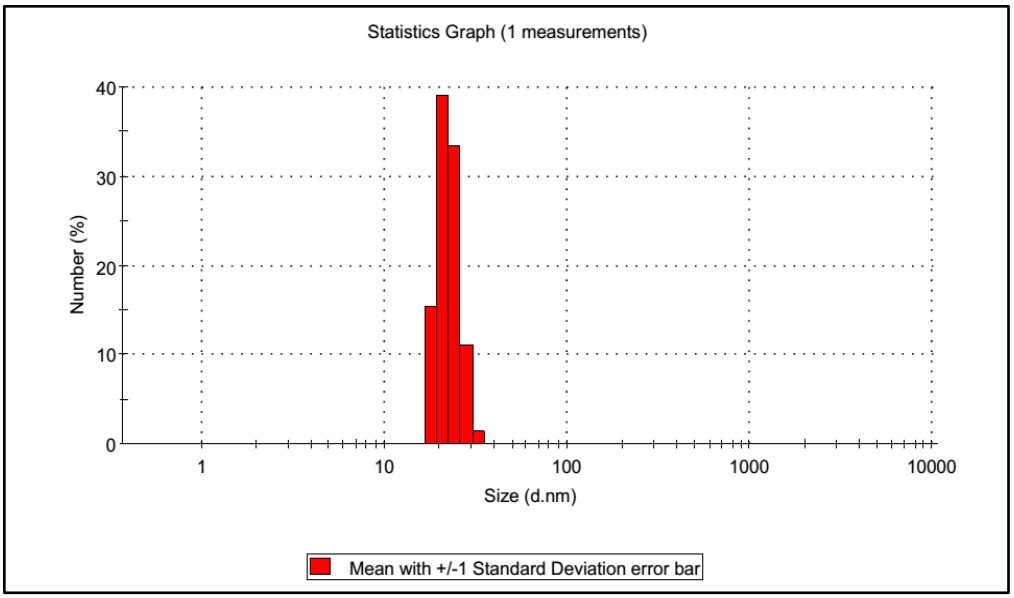

Figure 1: Particle size distribution of 8-hydroxyquinoline nanoparticles obtained by DLS analysis.

While SEM photomicrograph of air dried layer of 8-hydroxyquinoline nanoparticles is presented in Figure 2 which reveals distinct sphere clearly indicating the aggregated particles are spherical and relatively mono dispersed in shape. The average particles size estimated from SEM images is 200-300 nm and is relatively greater than the size obtained from DLS results. This is due to agglomeration of the nanoparticles during drying of suspension on glass substrate in an attempt obtain thin films.

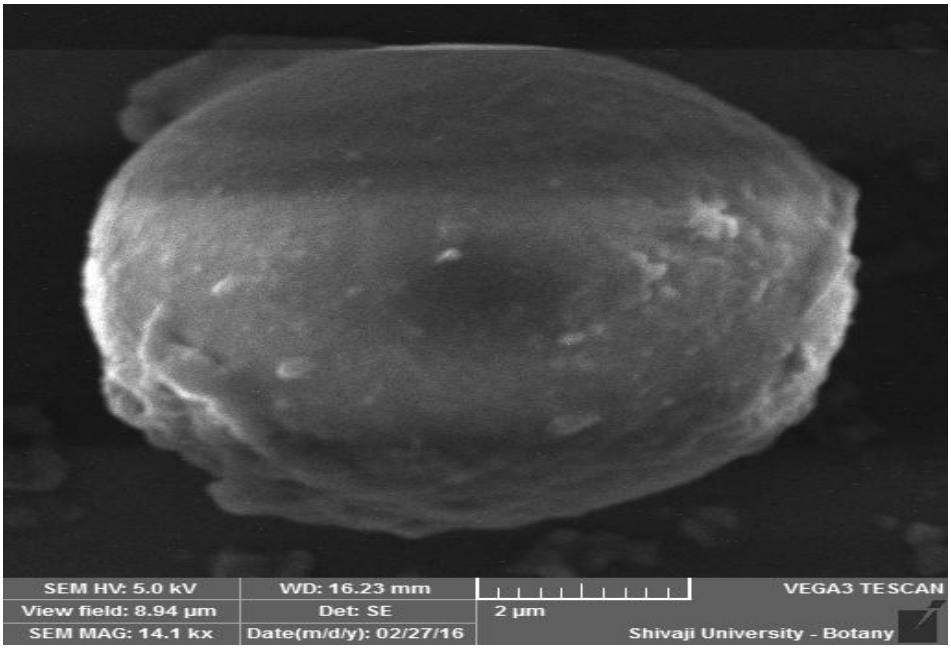

Figure 2: SEM photomicrograph of air dried layer of 8-hydroxyquinoline nanoparticles.

3.2 Photophysical properties of 8-hydroxyquinoline nanoparticles:

3.2.1 UV-visible spectroscopy:

The fluorescence and absorption properties of aqueous suspension of HQNPs are compared with spectral properties shown by the solution of sample of 8-hydroxyquinoline in acetone. Figure 3 presents absorption spectra (A) of acetone solution of 8-hydroxyquinoline and of aqueous suspension of its nanoparticles HQNPs (B). The absorption spectrum of HQNPs seen in Figure 3 is a broad band with maximum absorption at 242 nm and seen blue shifted from the absorption band of 8-hydroxyquinoline solution in acetone appeared with maximum absorption at 343 nm. The hypsochromic shift indicates that the 8-hydroxyquinoline molecules aggregate due to lateral π-stacking interactions. This observation led to consider formation of H-type aggregates in the water phase to give nanocluster of HQNPs.[51]

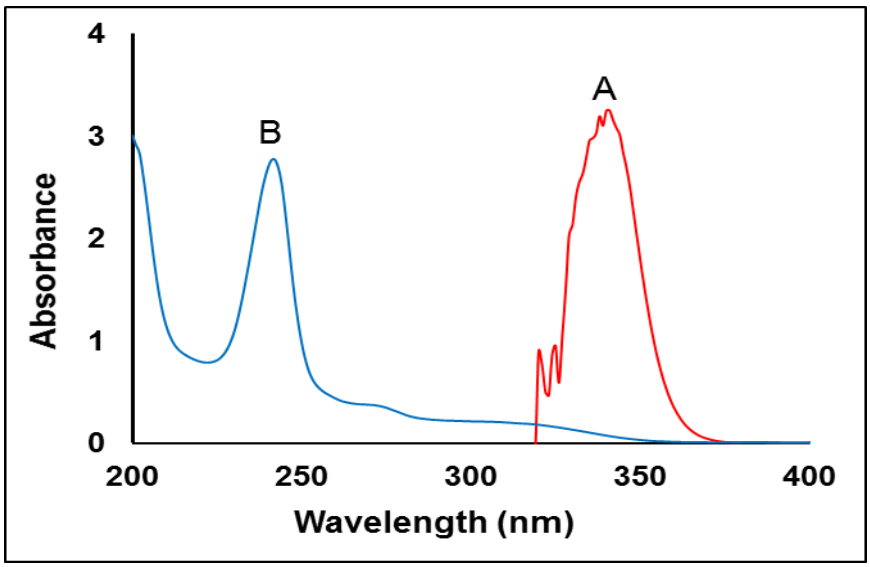

Figure 3: Absorption spectra of 8-hydroxyquinoline nanoparticles suspension (spectrum B) and 8-hydroxyquinoline solution in acetone (Spectrum A).

3.2.2 Fluorescence spectroscopy:

Excitation and fluorescence spectra of HQNPs suspension and that of the 8-hydroxyquinoline solution in acetone are shown in Figure 4. Excitation spectrum (A) of HQNPs is a broad band with maximum

fluorescence intensity λ_{ex} = 343 nm. In contrast excitation spectrum (B) of solution of 8-hydroxyquinoline is a sharp band peaking at 355 nm. The excitation spectrum of nanoparticles is blue shifted (Figure 4 A) from the excitation spectrum of 8-hydroxyquinoline by 12 nm. This observation is same with the hypsochromic shift noted in absorption spectra presented in Figure 3 and supports the consideration of H-aggregate formation by QZ molecules. The monomer emission is disappeared totally from the emission spectrum of nanostructure.

The fluorescence spectrum (D) of aqueous suspension of HQNPs is structureless broad band with maximum emission intensity at 527 nm. While the spectrum C of sample molecules 8-hydroxyquinoline in acetone solution is peaking at 423 nm. The fluorescence spectrum of nanoparticles is red shifted from the spectrum of sample molecules by about 104 nm. Such spectral shift in emission is always exhibited by the intermolecular interactions when molecules of similar type are closely packed and held by lateral π-stacking effects.

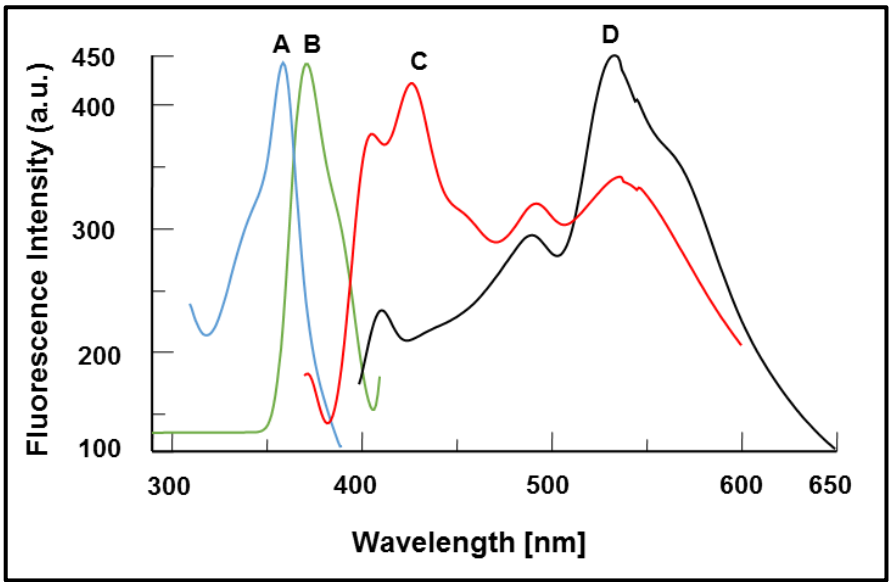

Figure 4: Excitation spectra of 8-hydroxyquinoline nanoparticles suspension (A), dilute solution of 8-hydroxyquinoline in acetone (B) and emission spectra of 8-hydroxyquinoline nanoparticles suspension (D), dilute solution of 8-hydroxyquinoline in acetone (C).

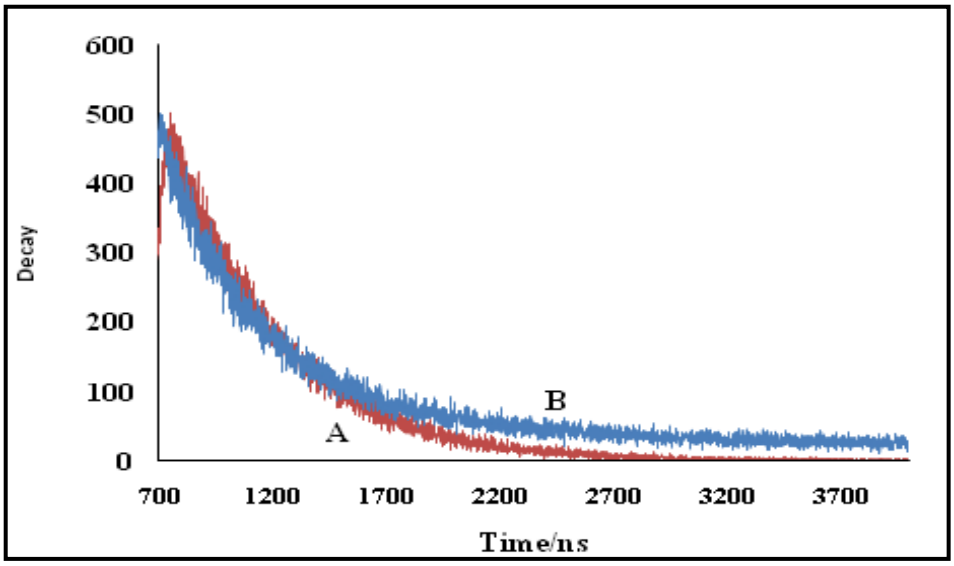

Figure 5: Fluorescence lifetime spectrum of dilute solution of 8-hydroxyquinoline in acetone (A) and 8-hydroxyquinoline nanoparticles suspension (B).

3.2.3 Fluorescence lifetime of HQNPs:

The fluorescence decay profile of dilute solution of 8-hydroxyquinoline in acetone monitored at λ_{ex} = 355 nm and λ_{em} = 423 nm and that of aqueous suspension of QZNPs monitored at λ_{ex} = 343 nm and λ_{em} = 527 nm are shown in Figure 5. The fluorescence lifetime 4.19 ns of HQNPs determined from the decay profile is longer than the lifetime 2.1 ns of dilute 8-hydroxyquinoline solution. The relatively long lifetime of nanoparticles indicate aggregation of the 8-hydroxyquinoline molecule to form nanostructure by self-assembly.

3.3 Effect of pH on fluorescence intensity of 8-hydroxyquinoline nanoparticles:

The variation in pH reflects changes in the molecular structure which ultimately leads into the disaggregation of nanoparticles. The effect of pH on fluorescence intensity of 8-hydroxyquinoline nanoparticles in aqueous suspension is illustrated in Figure 6 as bar diagram. It is evident from the figure that the colloidal stability of 8-hydroxyquinoline is seen to be maintained at pH of 8.0 with phosphate buffer. However, in low and high pH colloidal stability is affected and results into disaggregation of 8-hydroxyquinoline nanoparticles. Thus, the fluorescence intensity decreases.

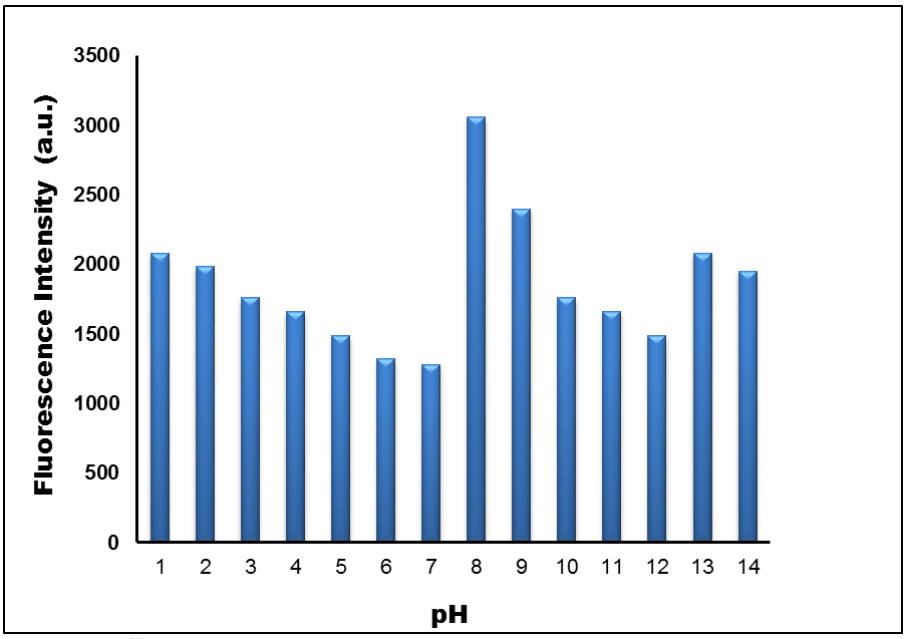

Figure 6: Effect of P^H on the fluorescence intensity (λ_{em} = 527 nm) of 8-hydroxyquinoline nanoparticles suspension (λ_{ex} = 343 nm).

3.4 Cation binding ability of the 8-hydroxyquinoline nanoparticles:

The spherical 8-hydroxyquinoline nanoparticles have negatively charged surface and hence can recognize cations. The cations recognition behavior was evaluated from changes in fluorescence intensity of 8-hydroxyquinoline nanoparticles upon addition of aqueous solution of salt of different cations. The fluorescence spectra of aqueous suspension of HQNPs maintained at pH = 8 by phosphate buffer were recorded in presence of Hg^{2+} and other interfering species such as Cu^{2+} Sn^{2+} Pb^{2+} Ca^{2+} Cd^{2+} Zn^{2+} Ni^{2+} K^{+} Na^{+} and Al^{3+} displayed in Figure 7. It is seen that presence of Hg^{2+} quenches fluorescence of HQNPs very significantly as compared to other interfering species.

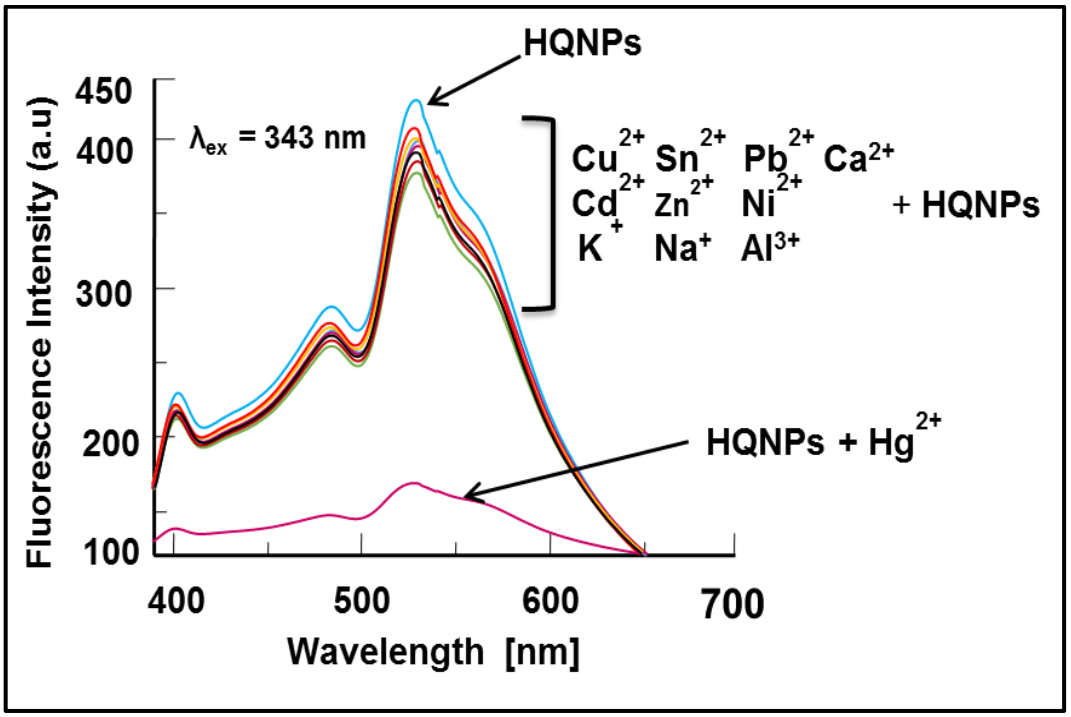

Figure 7: Selective fluorescence response of HQNPs towards Hg^{2+} (at λ_{ex} = 343 nm).

The selectivity of recognition of Hg^{2+} in presence of other interfering ions was examined by evaluating fluorescence intensity change $\Delta F/F = F_0\text{-}F/F$, where fluorescence intensity of HQNPs with Hg^{2+} and interfering ions and in absence of these species is F and F_0 respectively. The fluorescence intensity change of HQNPs containing Hg^{2+} and with different interfering species of concentration 5.00 µg.mL^{-1} each is presented in the form of bar diagram in Figure 8. The excitation wavelength used was 343 nm while fluorescence intensity of the mixture was noted at wavelength 527 nm, corresponding to maximum emission wavelength of HQNPs. The bar indicates that emission intensity change exhibited by Hg^{2+} remain unaffected even in presence of other interfering ions (blue bar) while coexisting ions without Hg^{2+} exhibited negligible change in the fluorescence intensity of HQNPs (red bar). This observation suggest that the HQNPs can selectively sense Hg^{2+} in presence of other species without any interference.

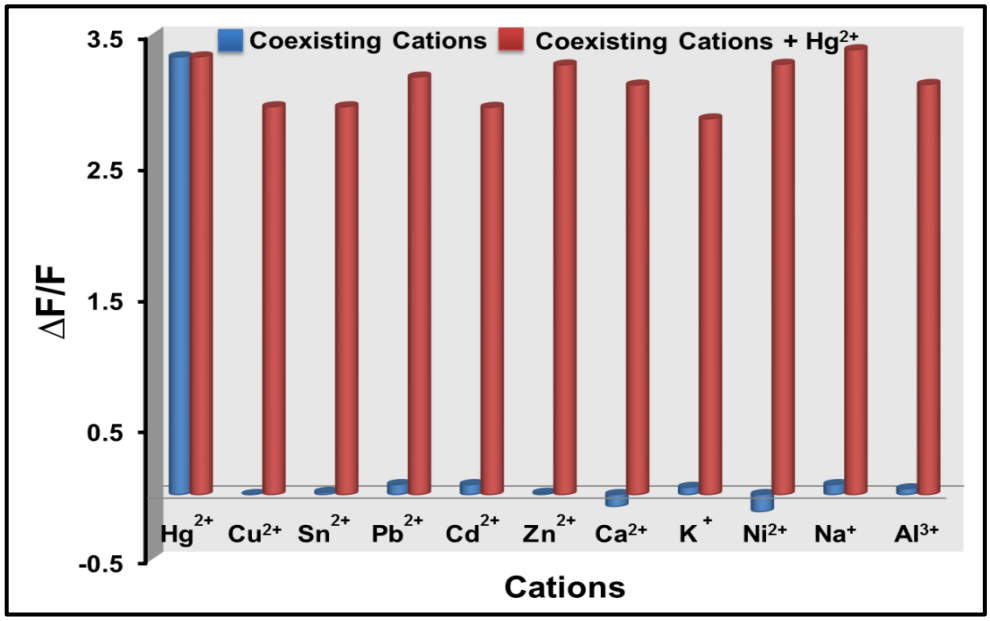

Figure 8: Fluorescence intensity change [ΔF/F] of the HQNPs solution in the presence and absence of Hg^{2+} and other coexisting substances with Hg^{2+} each of concentration 5.00 µg.mL^{-1}.

3.5 Fluorescence titration of HQNPs with Hg^{2+} ion solution:

Then series of mixture of solution were prepared by keeping volume of aqueous suspension of HQNPs constant to 1 mL and that of buffer solution to 2 mL, while the volume of Hg^{2+} ion solution was varies from 0.5 mL to 4.5 mL with increase by 0.5 unit and each mixture was diluted by water to total volume of 10 mL. The calculated concentration of Hg^{2+} solution is varies from 0.00 µg.mL^{-1} to 8.00 µg.mL^{-1}. The fluorescence spectra of all mixture were measured at λ_{ex} = 343 nm and overlayed in the Figure 9. The intensity noted at λ_{em} = 527 nm is the fluorescence intensity of HQNPs in presence of different concentration of Hg^{2+} solution in the range from 0.00 µg.mL^{-1} to 8.00 µg.mL^{-1}. The pH = 8 maintained by buffer was also checked by pH meter before the measuring the fluorescence spectra of mixture. From Figure 9 it is seen that increasing amount of Hg^{2+} solution decreases intensity of fluorescence gradually without any spectra modification.

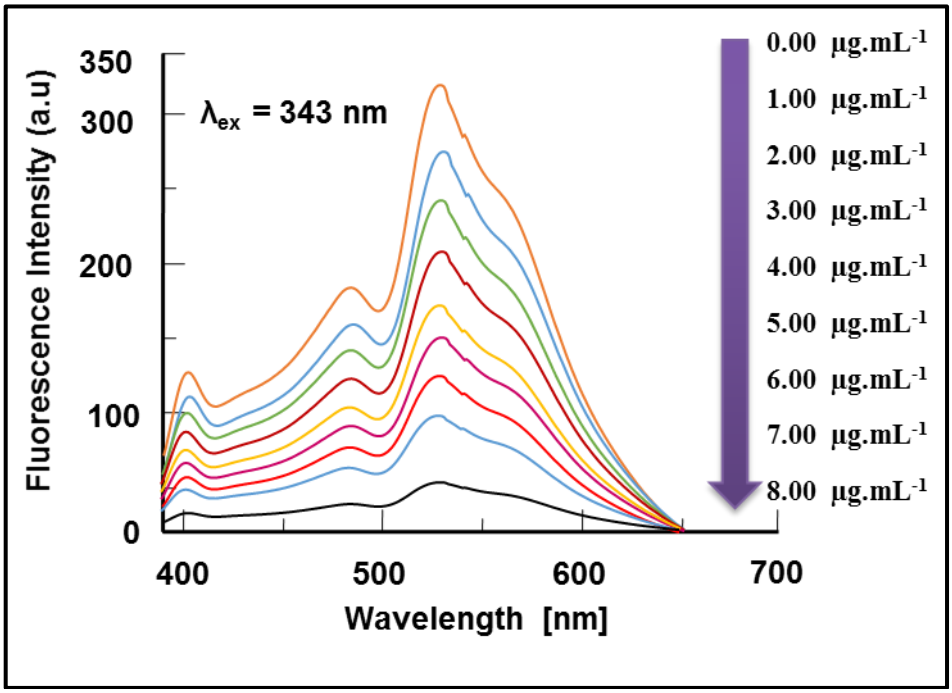

Figure 9: Fluorescence spectra of HQNPs suspension in the presence of different concentrations of aqueous solution of Hg^{2+} (0.00 µg.mL^{-1} to 8.00 µg.mL^{-1}) in Phosphate buffered (pH 8) at excitation wavelength λ_{ex} = 343 nm.

3.5.1 Validity of Stern-Volmer relation

The quenching results fit into the conventional linear Stern–Volmer equation.

$$\frac{Fo}{F} = 1 + K_{sv}[Q] \quad \ldots\ldots\ldots\ldots\ldots\ldots\ldots\ldots\ldots\ldots (1)$$

Where F_0 and F are the fluorescence intensity of the carbonate free 8-hydroxyquinoline nanoparticles suspension and suspension containing Hg^{2+} ion solution of concentration [Q] respectively. The Figure 10 shows the Stern-Volmer quenching line describing the F_0/F as a linear function of Hg^{2+} ion concentration. The coefficient of the linear fit is 0.992 and the Stern–Volmer quenching constant K_{SV} found to be 7.689 X 10^{11} M^{-1}. The limit of detection defined by the equation,

LOD = (3.3σ/k)…… (2)

Where σ is the standard deviation of the y-intercepts of regression lines and k is the slope of the calibration graph. The estimated LOD limit is 0.6920 µg.mL^{-1}. The detection limit is better than that of ordinary methods for the detection of Hg^{2+} ion.

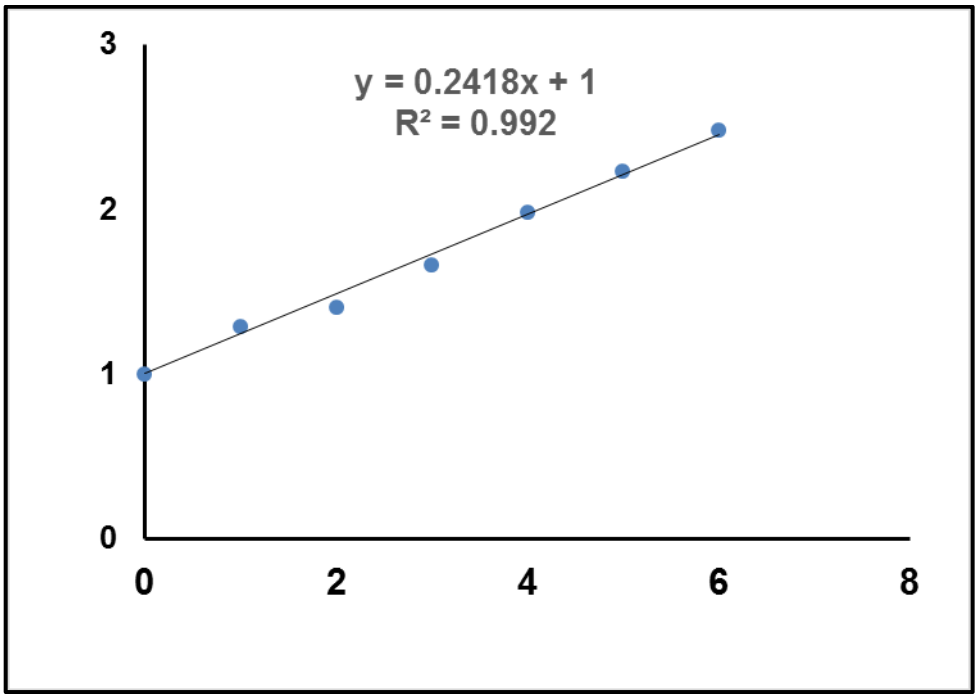

Figure 10: Stern-Volmer plot of fluorescence quenching data of 8-hydroxyquinoline nanoparticles to addition of different amount of Hg^{2+} ion solution.

3.6 Mechanism of fluorescence quenching:

In this work, it was observed that Hg^{2+} is strongly reacted with HQNPs to form metallic mercury. It means that, there could be strongly adsorption of freshly generated Hg^{2+} on the surface of HQNPs to form a metal-oxinate which could be responsible for the aggregation of HQNPs followed by the successive addition of Hg^{2+}, with fluorescence quenching. The plausible mechanism for fluorescence quenching is schematically represented in Scheme 1.

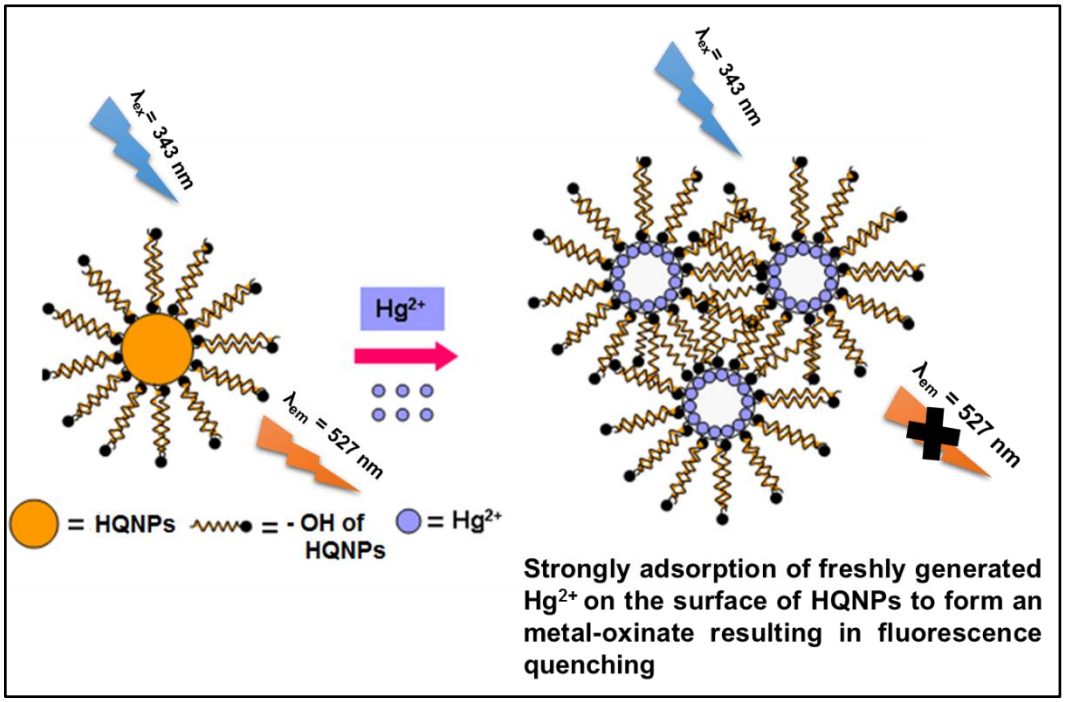

Scheme 1: Schematic illustration for aggregation of HQNPs with Hg^{2+}.

3.7 Development of HQNPs as a probe for the determination of mercury levels in waste water samples:

The method of sensing of Hg^{2+} by HQNPs based on fluorescence off approach was used to develop fluorimetric method of detection of Hg^{2+} in waste water sample collected from local region. The waste water samples collected from Ichalkaranji Industrial waste water (Kolhapur, MS, India) were first filtered through filter paper (Whatmann no. 41) to remove impurities. The filtered waste water samples were spiked with standard Hg^{2+} at two different concentration levels, then diluted to bring Hg^{2+} ion concentration within the working linear range and analyzed with the method proposed via a standard addition method. The accuracy and reliability of the method was further ascertained by recovery studies via a standard addition. The results are summarized in Table 1, which shows good consistency between the found values found by present method. These results demonstrate that the designed probe is applicable for fluorimetric detection of Hg^{2+} in environmental water samples without any interference.

Table 1: Determination of Hg^{2+} in waste water samples from different water sources by standard-addition method (n=3).

Waste water samples Studied*	Amount of standard Hg^{2+} added ($\mu g.mL^{-1}$)	Total Hg^{2+} Found (n=3) ($\mu g.mL^{-1}$)	Recovery of Hg^{2+} added (%)	RSD (%)	Relative error (%)
Ichalkaranji Industrial waste water (Kolhapur, MS, India)	2.5	2.84	101.58	0.25	1.58
	3.5	3.773	101.27	0.20	1.27

4. Conclusion:

8-Hydroxyquinoline nanoparticles prepared by the reprecipitation method can effectively recognize mercury ion over other co-existing ions in aqueous solution. The size distribution and surface morphology results have shown that the as prepared 8-hydroxyquinoline nanoparticles are monodispersed, small size and spherical in shape. The spectroscopy results indicated aggregation of 8-hydroxyquinoline molecules by self-assemble and the Aggregation Induced Enhanced Emission arising from nanoparticles. The quenching of fluorescence of nanoparticles due to the strong adsorption of freshly generated Hg^{2+} on the surface of HQNPs led to the development novel fluorimetric method for determination of sodium Hg^{2+} from the environmental waste water samples. The possible fluorescence quenching mechanism was also discussed. The method provides a fairly practical and economical approach. The objective of our work to prepare organic nanoparticles with specific charge on surface for recognition of ions is achieved and strategy can be extended further to achieve a long term goal of nanotechnology for the analytical processes.

5. References:

1 M. A. El-Sayed, *Acc. Chem. Res*., 34, **(2001)**, 257.
2 S. R. Emory, S. Nie, *J. Phys.Chem. B*, 102, **(1998)**, 493.
3 C. Templeton, D. E Cliffel, R. W Murray, *J. Am. Chem. Soc*., 121, **(1999)**, 7081.
4 M. Salerno, J. R. Krenn, B. Lamprecht, G. Schider, H. Ditlbacher, N. Felidj, A. Leitner, F. R. Aussenegg, *Opto-Electron.Rev.*, 10, **(2002)**, 217.
5 Y. Xia, P. Yang, Y. Sun, Y. Wu, B. Mayers, B. Gates, Y. Yin, F. Kim, H. Yang, *Adv. Mater.*, 15, **(2003)**, 353.
6 P. V. Kamat, *J .Phys .Chem. B*, 106, **(2002)**, 7729.
7 G. Maduraiveeran, R. Ramaraj, *Anal. Chem.*, 81, **(2009)**, 7552.
8 B. K. Jena, C. R. Raj, *Anal. Chem.*, 80, **(2008)**, 4836.

9 U. Kreibig, M Vollmer, *Optical Properties of Metal Clusters*, Springer, Berlin, **(1995)**.
10 M. Kerker, *The Scattering of Light and other Electromagnetic Radiation*, Academic Press, New York, **(1969)**.
11 C. F. Bohren, D. R. Huffman, *Absorption and Scattering of Light by Small Particles*, Wiley, New York, **(1983)**.
12 P. Mulvaney, *Langmuir* 12, **(1996)**, 788.
13 K. Aslan, J. R. Lakowicz, C. D. Geddes, *Anal. Biochem.* 330, **(2004)**, 145.
14 S. O. Obare, R. E. Hollowell, C. J. Murphy, *Langmuir*, 18, **(2002)**, 10407.
15 A. L. Gonzalez, C. Noguez, G. P. Ortiz, G. Rodriguez-Gattorno, *J. Phys. Chem. B*, 109, **(2005)**, 17512.
16 I. Onyido, A. R. Norris, E. Buncel, *Chem. Rev.* 104, **(2004)**, 5911.
17 N. Vasimalai, S. A. John *J. Lumin*, 131, **(2011)**, 2636.
18 A. H. Stern, *Environ. Res*,. 98, **(2005)**, 133.
19 Q. Wang, D. Kim, D. D. Dionysiou, G. A. Sorial, D. Timberlake, *Environ. Pollut*., 131, **(2004)**, 323.
20 F. A. Cotton, G. Wilkinson, C. A. Murillo, M. Bochmann, *Advanced Inorganic Chemistry, 6th ed*, John Wiley & Sons, New York, **(1999)**.
21 T. W. Clarkson, L. Magos, G. J. Myers, *N. Engl. J. Med*., 349, **(2003)**, 1731.
22 Y. Wang, F. Yang, X. Yang, *Biosens. Bioelectron*., 25, **(2010)**, 1994.
23 H .H. Harris, I. Pickering, G. N. George, *Science*, 301, **(2003)**, 1203.
24 P. Grandjean, P. Weihe, R. F. White, F. Debes, *Environ. Res*,. 77, **(1998)**, 165.
25 K. V. Gopal. *Neurotoxicol. Teratol*,. 25, **(2003)**, 69.
26 Y. Wang, F. Yang, X. Yang, *ACS Appl. Mater. Interfaces*, 2, **(2010)**, 339.
27 T. Lou, Z. Chen, Y. Wang, L. Chen, *ACS Appl. Mater. Interfaces*, 3, **(2011)**, 1568.
28 E. Y. Hashem, *Spectrochim. Acta A*, 58, **(2002)**, 1401.
29 A. Krata, W. Jedral, E. Bulska, *Spectrochim. Acta B*, 62, **(2007)**, 269.
30 A. M. Ashrafi, K. Vytras, *Talanta*, 85, **(2011)**, 2700.
31 X. Zhu, D. S. Alexandratos, *Microchem. J*, 86, **(2007)**, 37.
32 S. Ichinoki, N. Kitahata, Y. Fuji, *J. Liq. Chro-matogr. Rel., Technol*,. 27, **(2004)**, 1785.
33 B. Kuswandi, A. Nuriman, H. H. Dam, D. N. Reinhoudt, W. Verboom, *Anal. Chim. Acta.* 591, **(2007)**, 208.
34 A. Fan, Y. Ling, C. Lau, J. Lu, *Talanta*, 82, **(2010)**, 687.
35 J. S. Lee, A. K. R. L. Jean, S. J. Hurst, C. A. Mirkin, *Nano Lett.*, 7, **(2007)**, 2112.
36 M. Rex, F. E. Hernandez, A. D. Campiglia, *Anal. Chem.* 78, **(2006)**, 445.
37 Dynamic Light Scattering; Application Note by Malvern Instruments Ltd: Worcestershire, U. K., March 30, **(2012)**; http://www.malvern.co.uk.
38 Measuring Zeta Potential; Application Note by Malvern Instruments Ltd. Worcestershire, U. K., March 30, **(2012)**; http://www.malvern.co.uk.
39 M. Forough, K. Farhadi, *Turk. J. Eng. Environ. Sci.*, 34, **(2010)**, 281.
40 A. J. Bard, R. Parsons, J. Jordan, Standard Potentials in Aqueous Solution (*International Union of Pure and Applied Chemistry Marcel Dekker Inc., New York*, **(1985)**.
41 M. Katsikas, A. Gutie´rrez and J. Henglein, *Phys. Chem.*, 100, **(1996)**, 11203.
42 International Conference on Harmonization (ICH) of Technical Requirements for Registration of Pharmaceuticals for Human Use, *Topic Q2 (R1): Validation of Analytical Procedures: Text and Methodology*, 2005, www.ich.org.